

# Investigation of resonances in the total cross sections for excitation of mercury atoms by slow monoenergetic electrons

O. B. Shpenik, V. V. Souter, A. N. Zavilopulo, I. P. Zapesochnyĭ, and E. É. Kontrosh

*Uzhgorod State University*

(Submitted January 9, 1975)

*Zh. Éksp. Teor. Fiz.* 69, 48–58 (July 1975)

Precision studies have been made of the excitation of mercury atoms by slow electrons in an apparatus which included a trochoidal electron spectrometer. The energy dependence of the total cross sections for excitation of the twelve lowest energy levels has been studied with an electron energy spread of 0.04–0.14 eV. As the result of analysis of the structure of the excitation functions of the spectral lines by means of the Breit-Wigner and Fano formulas, fifteen resonances have been identified in the region of bombarding electron energies from 4.5 to 12.5 eV. The energies of the resonances have been determined and their widths have been estimated. The possible states of the negative mercury ion which resulted in appearance of the observed resonances are discussed.

PACS numbers: 34.70.D

## INTRODUCTION

Experimental and theoretical studies in recent years have shown that excitation of atomic levels can occur efficiently through compound states of the negative ion.<sup>[1]</sup> Contributions from negative ion states are observed in the collision cross sections in the form of resonances.

A large number of experimental investigations<sup>[2]</sup> have been devoted to study of the excitation of mercury atoms by electron impact. A detailed analysis shows that the formation of  $\text{Hg}^-$  compound states dominates the direct excitation of certain levels of mercury.<sup>[3-7]</sup> However, the existing experimental information on excitation of mercury is far from sufficient to determine the basic parameters of the resonances.

In this article we describe an apparatus with a trochoidal electron spectrometer, intended for study of the excitation of atoms by monoenergetic electrons both by optical and electrical methods, and we present the results of precision studies of resonances in the excitation cross sections of the mercury atom near threshold.

## APPARATUS

Resonances in the cross sections for collisions of electrons with mercury atoms have been the subject of study by two methods: by detection of the optical radiation of the excited atoms, and by analysis of the inelastically scattered electrons which have passed through the collision chamber. The apparatus developed and prepared for this purpose consists of a trochoidal electron spectrometer, a system for identification and detection of optical radiation, and a circuit to record the current of primary and scattered electrons.

The principal part of the apparatus, and one prepared for the first time, is the trochoidal electron spectrometer. It includes a trochoidal electron monochromator,<sup>[1]</sup> a collision chamber, and a trochoidal electron analyzer. A sectional schematic view of the spectrometer is shown in Fig. 1. An electron beam emitted by the oxide-coated cathode K is shaped by a system of diaphragms  $A_1$ ,  $A_2$ , and  $A_3$  in a longitudinal magnetic field. Dispersion in velocities arises as the result of the combined action of crossed electric and magnetic fields

between plates  $B_1$  and  $B_2$ . A monoenergetic beam of electrons is separated by the diaphragm in electrode  $A_4$ , accelerated to the necessary energy, passes through the collision chamber  $A_5$ , and hits the collector  $P_2$ . Between the vapor-filled cell  $A_5$  and the electron detector  $P_2$  is located the trochoidal electron analyzer ( $A_6$ ,  $A_7$ ,  $B_3$ ,  $B_4$ ), by means of which the energy distribution of the electrons in the beam is measured and the inelastically scattered electrons detected by the collector  $P_1$  are analyzed.

The spectrometer is placed in a metal vacuum chamber which is pumped by a diffusion pump with a pumping speed of 200 liters/sec with liquid nitrogen and zeolite traps. The entire system was baked at 400°C in high vacuum for 30–40 hours. The limiting pressure of residual gases in the vacuum chamber did not exceed  $(1-2) \times 10^{-7}$  Torr.

The trochoidal monochromator prepared by us permits the production of monoenergetic beam of electrons with a half-width in energy of 0.03 eV at a current of  $10^{-8}$  A. Comparison of the monochromator parameters measured by us with the theoretical predictions (see refs. 8 and 9) showed that the ratio of the half-width of the electron energy distribution to the theoretical value used in the design is in the range from 3 to 3.5. We note that the use of the trochoidal monochromator in the optical experiments provided a gain in intensity of the detected radiation from 2 to 10 times in comparison with electrostatic electron monochromators.

Radiation of the excited atoms was detected by a system for counting individual photoelectrons consisting of a photomultiplier with light flux modulation. This system has been described in detail previously.<sup>[10]</sup> Inelastically scattered electrons after analysis were recorded by an electrometer amplifier with a sensitivity of

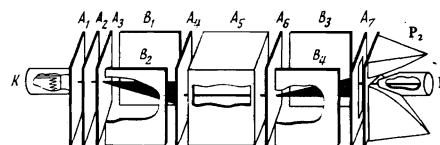


FIG. 1. Schematic sectional view of the trochoidal electron spectrometer.

$10^{-13}$  A. The analyzer was adjusted to transmit electrons which had lost an energy equal to the excitation energy of the level being studied.

## RESULTS AND ENERGY SCALE

We used the trochoidal monochromator in a careful study of the energy dependence of the total cross sections for excitation of the deepest singlet and triplet S, P, and D levels of mercury by detection of the optical radiation of the following spectral lines:  $\lambda$  2537 Å, 2803 Å, 3023/25/24 Å, 3132 Å, 3341 Å, 3650 Å, 4078 Å, 4108 Å, 4916 Å, 5461 Å, 5770 Å, and 5790 Å. We used the trochoidal spectrometer to study directly the excitation functions of the levels  $6^3P_0$ ,  $6^3P_1$ , and  $6^3P_2$  near threshold.

Some of the more interesting results are shown in Figs. 2–5. They were obtained with a mercury vapor pressure in the cell of  $(1-3) \times 10^{-3}$  Torr and an energy spread of the exciting electrons of 0.04–0.14 eV. In the figures shown the abscissa is the incident electron energy on an absolute energy scale, and the ordinate is a quantity proportional to the accumulated number of photomultiplier pulses (effective excitation cross section). The spread in the points in the ordinate at the peak of the curves, depending on the line intensity, was 2–5%. After averaging of five to seven measurements, this error was somewhat decreased and it is this quantity which is shown in the plots.

As can be seen from Figs. 2–5, in the measured excitation functions of most of the levels, a number of narrow maxima and minima—resonances—are observed. Before proceeding to analyze them, we will dwell on the question of calibration of the electron beam energy and the technique for determination of the location of the peaks in the excitation functions of the lines. In our experiments the calibration was accomplished on the basis of a primary reference standard, which we chose as the first narrow peak in the excitation function of the resonance transition of mercury (see Fig. 2). The location of

this peak in energy was determined by several means: by comparison of the initial part of the excitation function of the  $6^3P_1$  level (with allowance for the instrumental

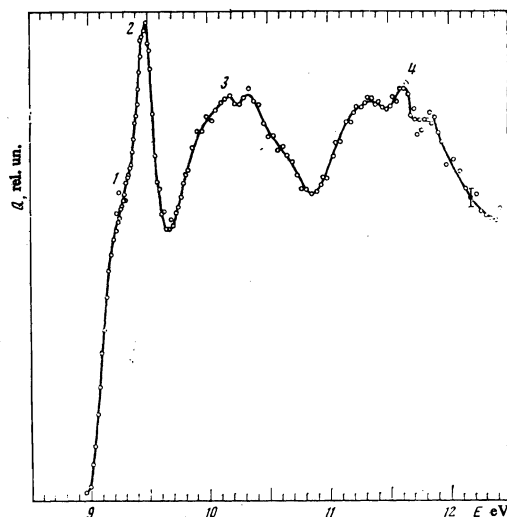


FIG. 3. Excitation function of the mercury line  $\lambda 3341$  Å ( $6^3P_2^0-8^3S_1$ ).

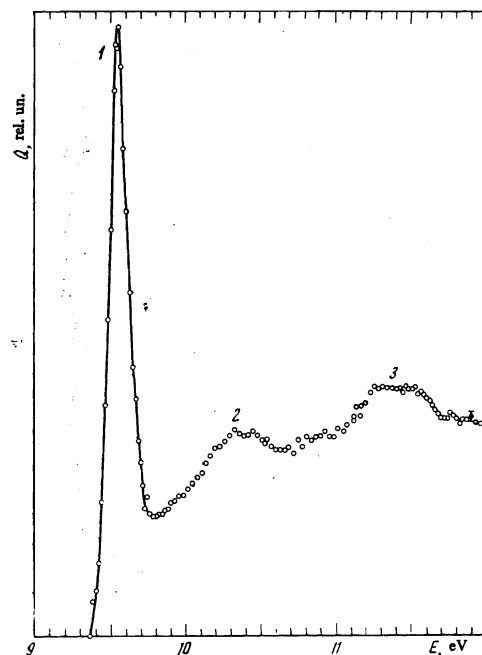


FIG. 4. Excitation function of the mercury line  $\lambda 3022/23/26$  Å ( $6^3P_2^0-7^3D_1$ ).

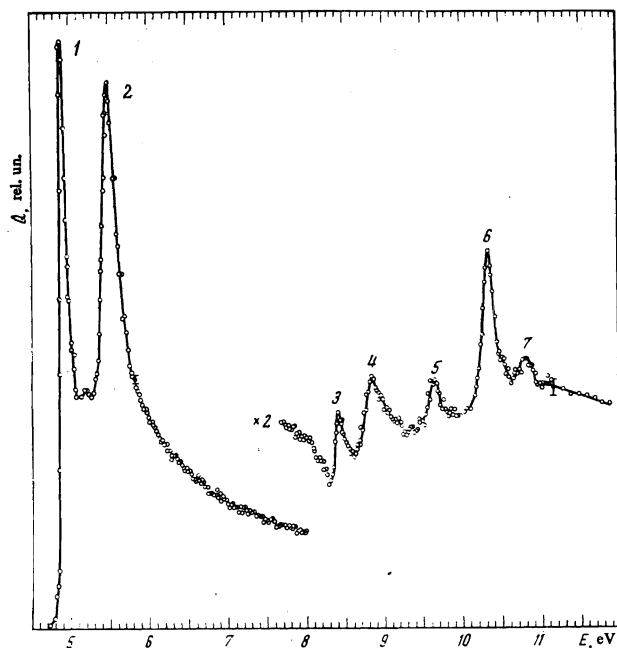


FIG. 2. Excitation function for the mercury resonance  $\lambda 2537$  Å ( $6^1S_0-6^3P_1^0$ ) ( $\times 2$  indicates increase of the coordinate scale by a factor of two).

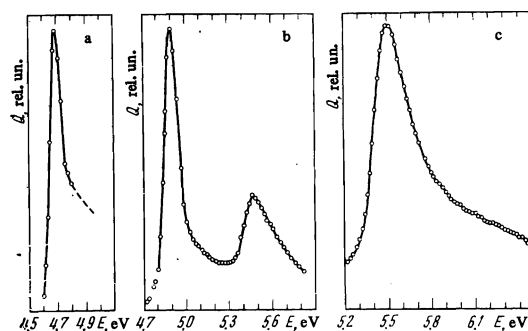


FIG. 5. Threshold behavior of the cross sections for excitation of the mercury levels  $6^3P_0^0$  (curve a),  $6^3P_1^0$  (curve b), and  $6^3P_2^0$  (curve c).

function measured by means of an analyzer<sup>2)</sup> with the excitation potential of the initial level of the line, from the shift in the volt-ampere characteristic of the electron current to the collector and the experimentally determined excitation thresholds of the lines,<sup>[3]</sup> and finally by the method of the half-width of the designed instrumental response function, proposed by Kurepa.<sup>[11]</sup> As the result of analysis of more than 50 measurements, it was established that the first peak in the excitation function of the line  $\lambda$  2537 Å is at  $E = 4.90 \pm 0.01$  eV. In experiments on passage of electrons through mercury vapor<sup>[5]</sup> at the same energy, a distinct resonance at  $E = 4.89 \pm 0.01$  eV was observed.

We note that the location in energy of the first peak in the excitation function of the  $6^3P_1$  level can serve as a reliable primary standard for absolute calibration of the energy of slow electron beams. The proposed new standard is easily determined, as a result of the large cross section for excitation of the  $6^3P_1$  level at this energy both by electrical and optical methods. Therefore it may turn out to be more convenient than the standard used up to this time (the resonance in helium at 19.35 eV).

We will discuss the means of determining the location of peaks in the excitation functions of the lines. Since the time for measurement of one curve amounted to 10–15 hours (the spacing between points was determined by the presence of singularities in the excitation function and was varied from 0.01 to 0.08 eV), this required special control of the stability of the experimental conditions. In particular, it was noted that the contact potential difference varied with time (from 0.01 to 0.03 eV in 5–6 hours of operation). This led to the necessity of taking into account the shift in the energy scale occurring during the course of the measurements. For this purpose we periodically (every two hours) checked the first peak in the excitation function of the  $\lambda$  2537 Å line and corrected the energy scale. As a result of this procedure, the accuracy in determination of the location of individual points on the energy scale of the excitation function being investigated was  $\pm 0.01$  eV. In determination of the accuracy in the position of the peaks and minima in each individual case, we also took into account the spread in points along the ordinate.

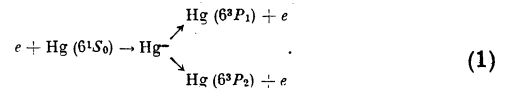
## DISCUSSION OF RESULTS

The fine structure in the optical excitation functions of mercury has been discussed repeatedly.<sup>[12–16]</sup> A detailed analysis of the new and extensive results obtained by us convinces us that, in addition to direct excitation of the initial levels from the normal state of the atom and cascade transitions, an important role in population of the levels of mercury is played by short-lived states of the mercury negative ion  $Hg^-$ .

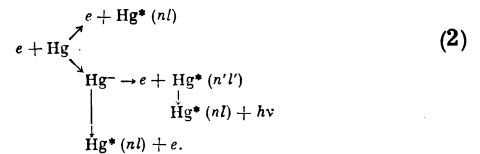
The role of the  $Hg^-$  levels appears most clearly in population of the  $6^3P_{012}$  levels in the near-threshold energy region. As can be seen from Fig. 5, the excitation functions of these levels are characterized by narrow peaks. In addition, the peak in the excitation function of the  $6^3P_1$  level at  $E = 5.49$  eV observed in the optical experiments is retained also in the electrical excitation function although its relative height turns out to be less.<sup>3)</sup> The shape and energy location of the second peaks in the electrical and optical excitation functions coincide.

Thus, we can conclude that the excitation function of the  $6^3P_1$  level near threshold is characterized by two

peaks, the distance between them agreeing within 0.02 eV with the energy interval between the  $6^3P_1$  and  $6^3P_2$  levels. This circumstance leads to the idea that the second peak in the excitation function of the  $6^3P_1$  level is associated with the  $6^3P_2$  level. Penkin and Redko<sup>[17]</sup> showed that in collisions of mercury atoms in  $6^3P_2$  states and  $6^1S_0$  states, the  $6^3P_1$  level is populated with a significant probability. However, we concluded that under the conditions of our experiment this mechanism does not play an appreciable role, since the excitation function of  $\lambda$  2537 Å remains unchanged as the mercury vapor pressure in the cell is changed over the range from  $3 \times 10^{-3}$  to  $1 \times 10^{-4}$  Torr. It appears to us that the origin of the second peak in the excitation function of the  $6^3P_1$  level and the peak in the excitation function of the  $6^3P_2$  level can be explained if we assume the existence in the immediate vicinity of the  $6^3P_2$  level of an  $Hg^-$  state whose decay with emission of an electron populates both the  $6^3P_1$  and  $6^3P_2$  levels:



Analysis of the observed structure in the excitation functions of other levels measured by us and of the structure at higher energies in the excitation function of the  $6^3P_1$  level is complicated by inclusion of the cascade mechanism of population of the initial levels of the lines. For example, certain peaks in the excitation function of the transition  $6^3P_2 - 7^2S_1$  transition practically coincide with the excitation energies of the  $7^3P_J$  and  $8^3P_J$  levels. We can suggest, taking into account the many-channel nature of the decay of negative ions, that the structure in the excitation function of the lines arises as a result of the following processes:



Therefore in what follows we will discuss our results from the point of view of the resonance approach, and will not be precisely concerned with what level the lines originated from (the initial level of the line or a level from which cascade transitions are possible).

It is well known that in the case of an isolated resonance the excitation cross section of an energy level can be described by the one-level Breit-Wigner formula<sup>[10]</sup>:

$$Q(E) = \frac{\pi}{k^2} \frac{\Gamma_0 \Gamma_1}{(E - E_0)^2 + \frac{1}{4} \Gamma^2}, \quad (3)$$

where  $k$  is the momentum of the incident electron,  $E_0$  is the resonance energy,  $\Gamma_0$  and  $\Gamma_1$  are respectively the half-widths of the elastic and inelastic decays, and  $\Gamma = \Gamma_0 + \Gamma_1$  is the total half-width of the resonance. When interference occurs between potential scattering (direct excitation of the level) and resonance scattering the cross section is described by the Fano formula<sup>[11]</sup>:

$$Q(E) = Q_r \frac{(q + \epsilon)^2}{1 + \epsilon^2} + Q_n, \quad (4)$$

where  $Q_r$  and  $Q_n$  are the resonance and nonresonance contributions to the cross section,  $q$  is the profile index, and  $\epsilon = (E - E_0)/(\Gamma/2)$ , where  $\Gamma$  is the half-width of the resonance.

In analysis of the results on the basis of Eqs. (4) and (3) to find the parameters of the resonance, it is neces-

sary to separate the potential part of the cross section  $Q_n$  (the background) from the resonance part. It is here that the main difficulty of the analysis arises. The point is that the shape of the cross section from nonresonance scattering is necessarily unknown. Nevertheless, if the resonance is sufficiently narrow, the variation in the background is comparatively easy to take into account. If the resonance is broad, then an incorrect account of the background will significantly distort the resonance shape. The analysis is further complicated by the fact that two or more resonances can partially overlap and, in addition, the measured curves are the result of folding of the excitation cross section of the levels and the instrumental resolution function. However, the optical method of investigation permits these difficulties to be overcome, since it is possible to obtain information on the same state of the negative ion ( $E_0$  and  $\Gamma$ ) leading to resonances with different  $q$  from the excitation functions of several spectral transitions.

We analyzed the results on the basis of the Fano and Breit-Wigner formulas as follows. In the excitation functions we separated the portions with the resonances and extrapolated the background (see Fig. 6) on the assumption that it varies smoothly with energy. Then, by subtracting the background from the experimental curve, we obtained the fold of the true resonance. The resonance location  $E_0$  was determined on the basis of the relation of Comer and Read<sup>[18]</sup>

$$\frac{h_2}{h_1} = \left| \frac{E_{min} - E_0}{E_{max} - E_0} \right|, \quad (5)$$

where  $h_2$  and  $h_1$  are the height of the maximum and the depth of the minimum relative to the wings of the resonance, and  $E_{max}$  and  $E_{min}$  are the energies at which the maximum and minimum of a given resonance are achieved. Then, defining  $q$  by the formula

$$q = \sqrt{h_2/h_1}, \quad (6)$$

and knowing the instrumental resolution function with which some excitation function was measured, we calcu-

lated the fold of this resolution function on the basis of Eq. (3) or (4) for various values of  $\Gamma$ . The true value of  $\Gamma$  was determined from the best agreement of the calculated folds with the experimentally observed resonance shape. As an example we have shown in Fig. 6 the result of the calculations in comparison with experiment. As can be seen, in the case of a narrow resonance (A and C) (the background does not greatly distort the shape), the agreement of the calculation with experiment is significantly better than for a broad resonance (B). In addition, poorer agreement of the calculations with experiment was observed for large values of  $q$ . This is explained by the large error in determination of  $h_1$  and  $h_2$ . Note that on analyzing the same resonance in different decay channels, we obtained values of  $E_0$  and  $\Gamma$  which were nearly the same. For example, on the basis of the excitation function of  $\lambda$  5461 Å ( $q = 2.9$ ),  $\lambda$  3341 Å ( $q = 1.3$ ), and  $\lambda$  3027 Å ( $q = 5.5$ ) we obtained respectively  $E_0 = 9.55$  eV,  $E_0 = 9.56$  eV, and in all three cases  $\Gamma = 0.06$  eV.

A summary of the data on calculated parameters of resonances in mercury, separated on the basis of the analysis described above,<sup>4)</sup> is given in the table. As can be seen, the resonance widths  $\Gamma$  lie in the range 0.03–0.60 eV. It is interesting to note that the same resonance is observed, as a rule, in several decay channels.

Estimates show that on the basis of the graphical analysis  $E_0$  is determined with an error which is not significantly greater than the error in determination of the location of the maxima in the excitation functions of the line,  $\pm 0.01$  eV– $\pm 0.08$  eV. The uncertainty in determination of the resonance width  $\Delta\Gamma/\Gamma$  is the range from 20% for resonances with  $\Gamma \geq 0.2$  eV to 60% for resonances with  $\Gamma \sim 0.1$  eV.

Let us now turn to discussion of the question of the possible states of the negative ion  $Hg^-$  leading to resonances in the excitation cross sections of the levels. The first attempt to identify states of the  $Hg^-$  negative ion

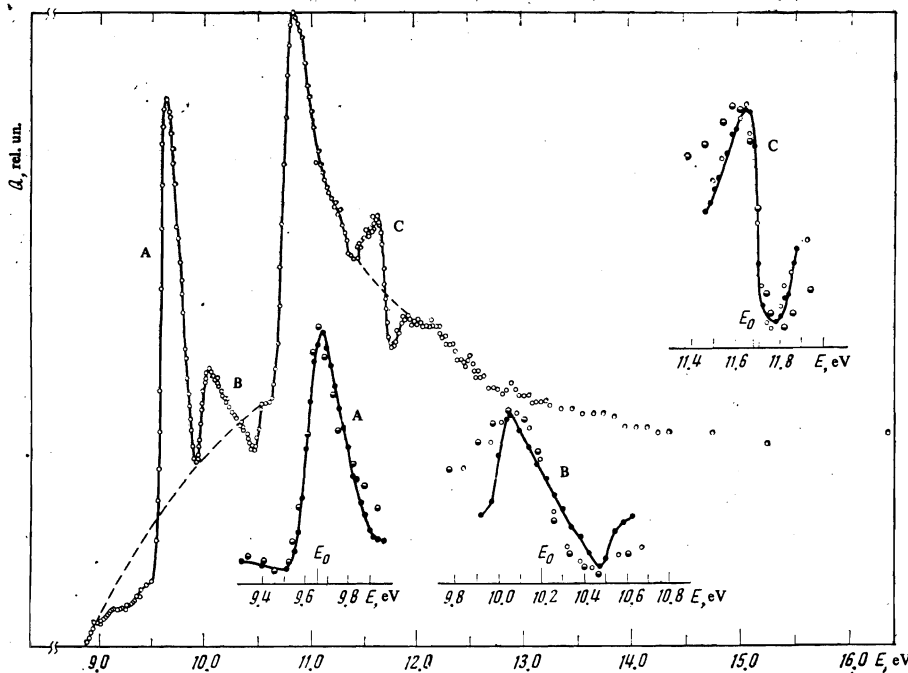


FIG. 6. Separated resonances in the excitation function of the line  $\lambda$  3650 Å in comparison with calculations according to Eq. (4). A— $q = 2.8$ ,  $\circ$ — $\Gamma = 0.06$  eV,  $\bullet$ —experiment; B— $q = 1.5$ ,  $\circ$ — $\Gamma = 0.14$  eV,  $\bullet$ —experiment,  $\circ$ — $\Gamma = 0.12$  eV; C— $q = -1$ ,  $\circ$ — $\Gamma = 0.08$  eV,  $\bullet$ —experiment,  $\circ$ — $\Gamma = 0.04$  eV.

Resonances		Levels in whose excitation function resonances are observed										
Location, $E_0$ , eV	Width $\Gamma$ , eV	$6^3P_0$	$6^3P_1$	$6^3P_2$	$7^3S_1$	$8^3S_1$	$6^3D_J$	$7^3D_J$	$6^1D_2$	$7^1S_0$	$8^1S_0$	$9^1S_0$
4.70±0.01	<0.1	×										
4.90±0.01	<0.1		×									
5.49±0.01	0.25		×	×								
8.18±0.06	0.6				×							
8.33±0.04	0.08		×							×		
8.62±0.04	<0.1			×								
8.80±0.03	0.24		×		×							
9.02±0.03	0.15				×							
9.56±0.03	0.06		×			×		×	×	×		
9.66±0.02	0.06						×					
10.20±0.08	0.2						×				×	
10.51±0.04	0.03				×		×					
10.90±0.06	0.3				×	×	×				×	×
11.50±0.03	0.04				×	×	×				×	
11.70±0.08	0.1				×	×	×				×	

was made by Fano and Cooper<sup>[6]</sup> in analysis of experiments on the passage of electrons through mercury vapor.<sup>[5]</sup> According to Fano and Cooper<sup>[6]</sup> the deepest states of  $Hg^-$  are  $^2S_{1/2}$ ,  $^2P_{1/2,3/2}$ ,  $^2D_{3/2,5/2}$ , and  $^4P_{1/2,3/2,5/2}$ , with electronic configuration  $5d^{10}6s6p^2$ . The fact that the three lowest resonances in the elastic channel correspond to  $Hg^-$  states  $5d^{10}6s6p^2$   $^4P_{1/2,3/2,5/2}$  (refs. 6 and 19) permits the conclusion that the resonances at 4.90 eV and 5.49 eV are due to  $5d^{10}6s6p^2$   $^2P_{1/2,3/2}$  states of  $Hg^-$ . This is confirmed by experiments on the polarization of  $\lambda$  2537 Å near threshold.<sup>[7]</sup>

As can be seen from the table, the resonance at ~8.20 eV appeared only in two decay channels—in the excitation functions of the levels  $7^1S_0$  and  $7^3S_1$ , and therefore we can write  $5d^{10}6s7s$   $^1S_07l$  and  $5d^{10}6s7s$   $^3S_17l$ . The lowest of these configurations is evidently the  $6s7s^2$   $^3S_{1/2}$  state of  $Hg^-$ , which leads to the resonance indicated.

The resonances in the region 8.34–9.02 eV and at 9.56 eV appear near the thresholds for excitation of the levels  $5d^{10}6s7p$   $^3P_{012}$ ,  $5d^96s^26p$   $^3P_2^0$ , and  $5d^{10}6s8p$   $^3P_{012}$  of mercury, these resonances being "shape resonances in all channels"<sup>[1]</sup> (see Figs. 2 and 3). We can therefore assume that the parents of these resonances are the electronic configurations  $5d^{10}6s7p$ ,  $5d^96s^26p$ , and  $5d^{10}6s8p$ . Addition of  $nl$  electrons to these states of the mercury atom gives the electronic configuration of the  $Hg^-$  ion. Just which states lead to the resonances discussed is hard to say. We can assume, however, that part of the structure in this energy region in the excitation functions of the  $7^3S_1$  and  $8^3S_1$  levels is the result of cascade transitions from the levels  $7^3P_J$ ,  $8^3P_J$ , and  $5d^96s6p$   $^3P_2^0$ . The latter are populated as the result of  $Hg^-$  decay. The resonance at  $E = 9.66$  eV, which is observed only in the excitation function of the  $6^3P_2-6^3D_J$  transition, may be due to  $Hg^-$  with an electron configuration  $5d^96s6pnl$ , whose decay leads to the  $5d^96s6p$   $^3P_1^0$  state of  $Hg$  with subsequent cascade population of the  $6^3D_J$  level. This is indicated by the fact that the resonance at  $E = 9.66$  eV is absent in the excitation function of the  $7^3D_J$  level, since the  $^3F_4^0$  level (excitation energy  $E = 9.53$  eV) lies 0.03 eV below the excitation energy of the  $7^3D_J$  level ( $E = 9.56$  eV).

The maxima located beyond the ionization threshold of the mercury atom ( $E_0$  of 10.90, 11.56, and 11.72 eV) are so-called Feshbach resonances,<sup>[1]</sup> since they are located directly below the displaced  $5d^{10}6p^2$   $^3P_0$  and Beutler  $5d^96s^26p$   $^3P_1$  and  $^3D_1$  levels. As can be seen from the table, they decay into many of the channels studied by us. Therefore we can suggest that resonances of this type arise as the result of formation of the  $5d^{10}6p^2nl$  and  $5d^96s^26pnl$  states of  $Hg^-$ .

## CONCLUSION

The experimental investigations carried out in the present work have shown that the trochoidal electron spectrometer is a universal tool for obtaining information on the mechanisms for population of atomic levels in collisions with slow electrons. Its advantages over other types of electron spectrometers are particularly evident in the study of total cross sections for excitation of atomic levels near threshold. Phenomenological analysis of the results obtained on excitation of the levels of the mercury atom has revealed the deeper mechanism of population of atomic levels and has identified three competing processes: direct transition of an electron from the ground state of the atom to an excited state, population of levels as the result of cascade transitions, and population through electron-atom compound states.

The authors express their gratitude to S. I. Biguntz, M. M. Dovganich, É. I. Meteleshko, and V. L. Ovchinnikov for their assistance in carrying out this work.

<sup>1</sup>This type of electron monochromator was developed by Stamatovič and Schulz.<sup>[8]</sup>

<sup>2</sup>Estimates of the broadening of the instrumental resolution function as the result of the Doppler effect give a value of  $3 \times 10^{-4}$  at  $E = 10$  eV.

<sup>3</sup>This is due to the change in the angular resolution of the analyzer with increase of the incident electron energy.

<sup>4</sup>Note that there are a number of other peaks; however, these were ignored in such an analysis of the experimental data, as a result of their insignificant contribution to the total cross section for excitation of the levels.

<sup>1</sup>G. J. Schulz, Rev. Mod. Phys. **45**, 378 (1973).

<sup>2</sup>L. J. Kieffer, Bibliography of low-energy electron collision cross-section data. N. B. S., Miscellaneous Publication, 1967, p. 280.

<sup>3</sup>I. P. Zapesochnyi and O. B. Shpenik, Zh. Eksp. Teor. Fiz. **50**, 890 (1966) [Sov. Phys.-JETP **23**, 592 (1966)].

<sup>4</sup>C. Smit and H. M. Fijnaut, Phys. Lett. **19**, 121 (1965).

<sup>5</sup>C. E. Kuyatt, J. A. Simpson, and S. R. Mielczarek, Phys. Rev. **138**, A385 (1965).

<sup>6</sup>U. Fano and J. W. Cooper, Phys. Rev. **138**, A400 (1965).

<sup>7</sup>T. W. Ottley, D. R. Denne, and H. K. Kleinpoppen, Phys. Rev. Letters **29**, 1646 (1972). B. L. Fedorov and A. P. Mezentsev, Opt. Spektrosk. **19**, 12 (1965) [Opt. Spectrosc.].

<sup>8</sup>A. Stamatovič and G. J. Schulz, Rev. Sci. Instr. **41**, 423 (1970).

<sup>9</sup>D. Roy, Rev. Sci. Instr. **43**, 535 (1972).

<sup>10</sup>O. B. Shpenik, I. P. Zapesochnyi, V. V. Souter, E. É. Kontrosh, and A. N. Zavilopulo, Zh. Eksp. Teor. Fiz. **65**, 1797 (1973) [Sov. Phys.-JETP **38**, 838 (1974)].

<sup>11</sup>J. M. Kurepa, Doctoral dissertation, Physics Institute, Belgrade, 1972.

<sup>12</sup>S. E. Frish and I. P. Zapesochnyi, Dokl. Akad. Nauk SSSR **55**, 971 (1954).

<sup>13</sup>I. P. Zapesochnyi, Vestnik (Bulletin) Leningrad State University **1**, 67 (1954).

<sup>14</sup>H. M. Jongerius and J. A. Smit, Appl. Sci. Res. **5**, 59 (1955); H. M. Jongerius, Van Egmond, and J. Smit, Physica **9**, 22, 845 (1956).

<sup>15</sup>S. É. Frish, and A. N. Klyucharev, Opt. Spektrosk. **22**, 174 (1967) [Opt. Spectrosc.]. R. J. Anderson, E. T. P. Lee, and C. C. Lin, Phys. Rev. **157**, 31 (1967).

<sup>16</sup>I. P. Bogdanova and V. D. Marusin, Opt. Spektrosk. **20**,

209 (1966) [Opt. Spectrosc.]. I. P. Bogdanova and V. D. Marusin, Opt. Spektrosk. 21, 252 (1966) [Opt. Spectrosc.]. I. P. Bogdanova and V. E. Yakhontova, Opt. Spektrosk. 22, 14 (1967) [Opt. Spectrosc.].  
<sup>17</sup>N. P. Penkin and T. P. Redko, VIII ICPEAC, Abstracts of Papers, 333, Belgrade, 1973.

<sup>18</sup>J. Comer and F. H. Read, J. Phys. E5, 211 (1972).  
<sup>19</sup>M. Duweke, N. Kirchner, E. Reichert, and E. Stuaadt, J. Phys. B6, 1208 (1973).

Translated by C. S. Robinson  
5